

Electron-hole excitations in Mg_2Si and Mg_2Ge compounds

B. Arnaud and M. Alouani

*Institut de Physique et de Chimie des Matériaux de Strasbourg (IPCMS), UMR 7504 du CNRS–Université Louis Pasteur,
23 Rue du Loess, 67037 Strasbourg Cedex, France*

(Received 6 February 2001; published 27 June 2001)

The recently implemented all-electron GW approximation shows that the conduction band quasiparticle energies of Mg_2Si and Mg_2Ge compounds are shifted by a constant energy Δ toward higher energies compared to the local-density approximation results whereas the valence bands remain unchanged. Including excitonic effects considerably improves the optical spectra peak positions and their intensities obtained within the random-phase approximation. The calculation predicts a low energy structure that is present in the experimental optical spectrum of Mg_2Ge but remains to be observed for Mg_2Si .

DOI: 10.1103/PhysRevB.64.033202

PACS number(s): 71.15.Mb, 78.20.Ci

The electronic structure of conventional semiconductors is well described by means of the so-called GW approximation of Hedin.¹ In this approximation the electron self-energy operator is approximated by the product of the Green's function G and the screened Coulomb interaction W and the calculation is *not* self-consistent. It was argued, at least in the case of a homogeneous electron gas, that this success is due to a strong compensation between the vertex corrections and the effect of the self-consistency.² Nevertheless, this issue is still debated in the literature, and recent calculations by Ummels *et al.*³ show that, while the first-order vertex and the self-consistency corrections to the polarizability cancel each other, this is not the case for the first-order corrections to the GW gap of silicon and germanium. It was also argued by Farid that the excitation energies of an inhomogeneous interacting system cannot be achieved without including the vertex part of the self-energy.⁴

Because it is computationally difficult to perform truly self-consistent *ab initio* quasiparticle (QP) calculations including vertex corrections it is crucial to study a variety of compounds within the GW approximation to determine the validity and limitations of this successful approximation. Furthermore, an accurate knowledge of the QP excited states is a necessary ingredient for the determination of the optical spectra of materials. Indeed, it was shown by several groups, using *ab initio* pseudopotential^{5–7} and more recently an all-electron basis set,⁸ that the discrepancy between the theoretical and experimental optical spectra is recovered when the QP energies and the electron-hole interaction are included in the calculation. These advances in computational physics have triggered further interest in *ab initio* computation of optical properties of materials. In particular, the GW approximation together with the Bethe-Salpeter equation (BSE) has been used to study the optical spectra of conventional semiconductors,^{5–9} conjugated polymers,^{10,11} insulators,^{6,7} hydrogenated Si clusters,¹² α -quartz,¹³ the Ge(111)- 2×1 surface,¹⁴ and molecules.¹⁵

In this Brief Report, we extend the all-electron GW approximation and the BSE to study the effects of correlations on the electronic properties of Mg_2Si and Mg_2Ge as well as the local-field and electron-hole interaction effects on their optical spectra. Mg_2Si and Mg_2Ge are semiconductors having the antifluorite structure¹⁶ and can be viewed as superlat-

tices of alternating metallic Mg and semiconducting Si or Ge monolayers, respectively. These compounds are of interest because they form the simplest metal-semiconductor hybrid materials, and determination of their optical properties represents the first extension beyond the study of the zincblende semiconductor class of materials. Their energy band gaps are relatively small leading to interband transitions in the visible region. The optical properties of these materials were extensively studied in the late 1960s;^{16–19} unfortunately only empirical pseudopotential calculation of the electronic structure and the dielectric function have been attempted by Au-Yang and Cohen.²⁰

In this study we used our recently implemented GW approximation¹ in conjunction with the all-electron full-potential projector augmented wave (PAW) method²¹ to determine the electronic structure and the dielectric function of these compounds. Our method has been previously used with success to compute the electronic structure of some small-, medium-, and large-band-gap semiconductors.²² We have shown that the GW -PAW method accounts for most of the discrepancy between the local-density approximation (LDA) and experiment regarding the energy positions of the conduction states. The extension of this method to compute the optical spectra of semiconductors including the local-field effects and the electron-hole interaction has also been a great success, since the results compared nicely with the optical spectra of semiconductors.⁸ The dynamical dielectric function is computed with and without the local-field and electron-hole interaction effects. The conduction state QP energies are assumed to be the LDA eigenvalues shifted by a constant energy Δ calculated by means of the GW approximation. As will be shown later, this is a good approximation since the GW band structure along the high symmetry direction can be produced from the LDA results by adding the energy shift Δ to the LDA conduction states. Furthermore, the optical spectra of Si and diamond obtained using the GW QP energies were almost identical to those obtained using shifted LDA energies.⁸

Quasiparticles within the GW approximation. As described elsewhere²² we can find the excitation energies of a material by solving a QP equation instead of locating the poles of the Green's function. After calculating the matrix elements of the self-energy operator $\Sigma(\mathbf{r}, \mathbf{r}', \epsilon_{nk}^{qp})$ between

TABLE I. Quasiparticle lowest energy band gaps of Mg₂Si and Mg₂Ge in eV compared to the LDA results and experiment.

	LDA	<i>GW</i>	Expt. ^a
Mg ₂ Si			
Γ _{15v} →Γ _{1c}	1.55	2.20	2.1
L' _{3v} →L _{3c}	3.17	3.76	3.7
X' _{5v} →X _{1c}	2.19	2.85	2.5
Γ _{15v} →X _{1c}	0.12	0.65	0.66–0.78 ^b
Mg ₂ Ge			
Γ _{15v} →Γ _{1c}	0.90	1.63	1.6
L' _{3v} →L _{1c}	1.47	2.23	2.1
L' _{3v} →L _{3c}	3.29	3.92	4.1
Γ _{15v} →X _{1c}	0.03	0.50	0.57–0.74 ^c

^aReference 17 unless otherwise indicated.

^bReference 18.

^cReference 19.

LDA orbitals, the QP energies ϵ_{nk}^{qp} are determined using a first-order perturbation theory to the QP equation,

$$\epsilon_{nk}^{qp} = \epsilon_{nk}^{LDA} + \langle \Psi_{nk} | \Sigma(\mathbf{r}, \mathbf{r}') | \Psi_{nk} \rangle - \langle \Psi_{nk} | V_{xc}^{LDA}(\rho_v(\mathbf{r})) | \Psi_{nk} \rangle,$$

where ϵ_{nk}^{LDA} and Ψ_{nk} are the LDA eigenvalues and wave function, respectively, and V_{xc}^{LDA} is the LDA exchange-correlation potential for valence electrons of density ρ_v . In the *GW* approximation, Σ is approximated by a convolution with respect to the frequency variable of the Green's function G , with the screened interaction W calculated within the random-phase approximation (RPA). Usually the LDA eigenvalues are used in G ; however, we have found that when updating the energies in G by the first estimated QP energies, the *GW* approximation provides QP energies that are in better agreement with experiment.⁸ Thus, the calculated QP band gaps, using the updated G , are slightly larger than those reported earlier²² for Mg₂Si.

The Mg₂X compounds, where X=Si or Ge, are semiconducting and crystallize in the antifluorite structure. The primitive unit cell contains an X atom at the (0,0,0) position and two equivalent Mg atoms at the (a/4)(111) and (3a/4)(111) positions, where a is the lattice parameter. Band structure calculations were performed using the experimental lattice parameters of 6.39 Å and 6.378 Å for Mg₂Si and Mg₂Ge, respectively. A cutoff energy of 20 Ry for the expansion of the plane waves was used, which corresponds to 645 reciprocal lattice vectors, and it is found to be sufficient for the convergence of the LDA results. The *GW* QP energies were obtained using the plasmon-pole model of Engel and Farid.²³ The model parameters were determined by diagonalizing 331×331 polarizability matrices. We found that two special \mathbf{k} points and 200 bands are enough for the convergence of the QP energies.

Table I compares the LDA, the *GW* approximation, and the experimental results for the direct and indirect band gaps at Γ, X, and L of Mg₂X compounds. In the absence of a photoemission experiment, the calculations are compared to

the experimental results deduced from the reflectivity spectra,¹⁷ despite the fact that the experimental results include excitonic effects. In both the LDA and the *GW* approximation, the maximum of the valence states is at Γ whereas the minimum of the conduction states is at X, which makes these compounds indirect-band-gap semiconductors, in good agreement with experiment. The size of the band gap is well reproduced by the *GW* method for the Mg₂Si compound; however, it is slightly underestimated for the Mg₂Ge compound. It is important to mention that the spin-orbit coupling has been ignored in our calculation. This seems to be a good approximation since the splitting of the Γ_{15v} is estimated¹⁷ to be only about 0.03 eV for Mg₂Si, and 0.2 eV for Mg₂Ge. In the latter, the spin-orbit coupling slightly reduces the *GW* approximation band gap, worsening the agreement with experiment at the 0.1 eV level.

When calculating the band structures of Mg₂Si and Mg₂Ge along the high symmetry direction we noticed that the valence bands are almost unchanged in both calculations whereas the *GW* conduction bands can be deduced from the LDA bands by a rigid energy shift Δ over the whole Brillouin zone. The Δ values that can be extracted from the band structure plots are 0.62 eV and 0.70 eV for Mg₂Si and Mg₂Ge, respectively. These values are used to correct the LDA eigenvalues to be used in the calculation of the dielectric function of these compounds.

Local field and excitonic effects. The calculation of the dielectric function is done as described in our recent paper.⁸ Here we outline the method of calculation that includes the local-field effects and the electron-electron interaction. First, the electron-hole amplitudes $A_{vc\mathbf{k}}^\lambda$ and the excitation energies E^λ are obtained by solving an effective two-particle Schrödinger equation, which originates from the BSE,²⁴

$$(\epsilon_{c\mathbf{k}}^{qp} - \epsilon_{v\mathbf{k}}^{qp})A_{vc\mathbf{k}}^\lambda + \sum_{v'c'\mathbf{k}'} [2 \Xi_{vc\mathbf{k},v'c'\mathbf{k}'}^{exch} \delta_{s,0} + \Xi_{vc\mathbf{k},v'c'\mathbf{k}'}^{dir}] A_{v'c'\mathbf{k}'}^\lambda = E^\lambda A_{vc\mathbf{k}}^\lambda,$$

where $\Xi_{vc\mathbf{k},v'c'\mathbf{k}'}^{exch}$ are the exchange matrix elements (present for singlet excitons, $s=0$, only) of the bare Coulomb interaction \bar{v} without the long range term of vanishing wave vector

$$\Xi_{vc\mathbf{k},v'c'\mathbf{k}'}^{exch} = \int d\mathbf{r}d\mathbf{r}' \Psi_{v\mathbf{k}}(\mathbf{r}) \Psi_{c\mathbf{k}}^*(\mathbf{r}) \bar{v}(\mathbf{r}, \mathbf{r}') \times \Psi_{v'\mathbf{k}'}^*(\mathbf{r}') \Psi_{c'\mathbf{k}'}(\mathbf{r}'),$$

and $\Xi_{vc\mathbf{k},v'c'\mathbf{k}'}^{dir}$ are the matrix elements of the static screened interaction W calculated within the RPA

$$\Xi_{vc\mathbf{k},v'c'\mathbf{k}'}^{dir} = - \int d\mathbf{r}d\mathbf{r}' \Psi_{v\mathbf{k}}(\mathbf{r}) \Psi_{c\mathbf{k}}^*(\mathbf{r}') W(\mathbf{r}, \mathbf{r}', \omega=0) \times \Psi_{v'\mathbf{k}'}^*(\mathbf{r}) \Psi_{c'\mathbf{k}'}(\mathbf{r}').$$

The relevant parameters of our calculations are the number of valence bands N_v , the number of conduction bands N_c , and the number of \mathbf{k} points $N_{\mathbf{k}}$. The set of \mathbf{k} points belong to

a regular grid that is rigidly shifted slightly from the high symmetry planes of the Brillouin zone. The small symmetry breaking vector produces converged spectra with a limited number of \mathbf{k} points by avoiding degenerate eigenstates.

The numerical effort for solving the BSE is large, because the basis set for the electron-hole wave functions has at least 10^4 functions, which brings the number of matrix element $\Xi_{vc\mathbf{k},v'\mathbf{k}'}$ to 10^8 . For a system where the number of valence bands is N_v , the number of conduction bands is N_c , and the number of Brillouin zone points is N_k , the number of matrix elements to be evaluated is $[N_v \times N_c \times N_k]^2$. For example, for Mg_2Si , with three valence bands and four conduction bands, we need up to 512 \mathbf{k} points and a lifetime broadening of 0.24 eV to obtain a good optical spectrum. The inclusion of the excitonic effects in the optical spectrum of Mg_2Si necessitates the evaluation of 3.8×10^7 matrix elements. This number can be reduced to 1.9×10^7 by using the Hermiticity of the Hamiltonian matrix. This Hamiltonian is then diagonalized to obtain the eigenvectors A^λ and eigenvalues E_λ that are necessary for the calculated imaginary part of the dielectric function

$$\epsilon_2^{(2)}(\omega) = \lim_{\mathbf{q} \rightarrow 0} \frac{4\pi}{\Omega} \times \frac{1}{\mathbf{q}^2} \times \sum_{\lambda} \left| \sum_{vc\mathbf{k}} \langle v\mathbf{k} | e^{-i\mathbf{q}\cdot\mathbf{r}} | c\mathbf{k} \rangle A_{vc\mathbf{k}}^{\lambda} \right|^2 \times \delta(E_{\lambda} - \omega).$$

Results and discussion. The Mg_2X ($X=\text{Si}$ or Ge) compounds are characterized by large static dielectric functions ϵ_{∞} . We inverted the dielectric functions directly to determine their static dielectric function. The LDA without local-field effects produces values of 18.4 and 19.01 for Mg_2Si and Mg_2Ge , respectively. When the local-field effects are included these values are drastically reduced to 13.71 and 13.62, respectively. Thus the local-field effects bring these results in to better agreement with the experimental results¹⁶ of 12.9 and 13.3.

Figure 1 shows our calculated dielectric function including the local-field and excitonic effects for Mg_2X ($X=\text{Si}$ or Ge) compared to the RPA dielectric function and to the experimental results of Scouler.¹⁶ The limitation of the number of conduction bands is dictated by the large size of the excitonic Hamiltonian. The RPA optical spectra show three pronounced structures that we labeled E_1 , E_2 , and E_3 by increasing photon energy [see Fig. 1]. The onset of absorption E_0 is associated with the $\Gamma_{15} \rightarrow \Gamma_1$ transition of about 2.2 eV for Mg_2Si and 1.63 eV for Mg_2Ge . The tail below the onset of absorption is due to the lifetime broadening effect which mimics the self-energy contribution. The three structures in the optical spectra, by increasing photon energy, are associated with the following interband transitions across the Brillouin zone: $L'_3 \rightarrow L_1$, $(X'_5 \rightarrow X_1$ and $X'_5 \rightarrow X_3)$, and $L'_3 \rightarrow L_3$, respectively. The assignment of the origin of the peaks is in good agreement with the empirical PP calculation of Au-Yang and Cohen. The positions of the peaks are shown in Table II and are found to be in a fairly good agreement with experiment. It is worth mentioning that our calculation of the excitonic effects shows that the main peak is shifted by about 0.2 eV toward lower photon energies for both compounds in

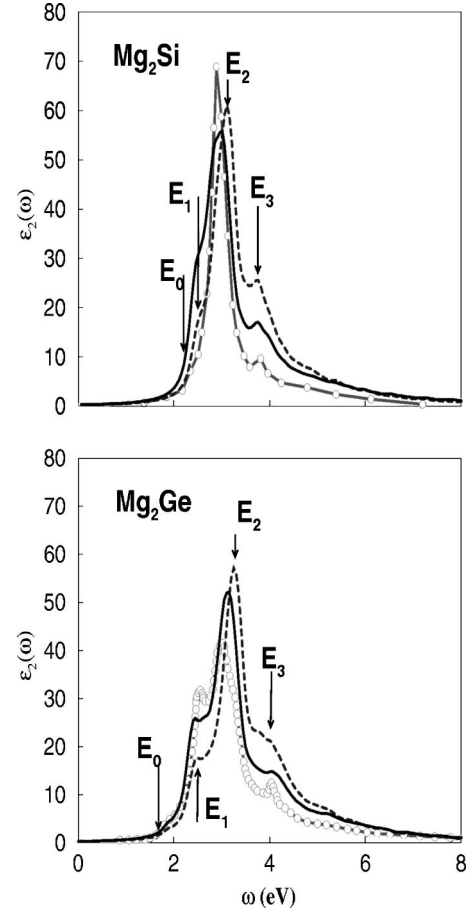


FIG. 1. Calculated imaginary part of the dielectric function of Mg_2Si and Mg_2Ge within the RPA (dashed curve) and including both the local-field effects and e - h interaction (solid curve) compared to the experimental spectrum (Ref. 16).

good agreement with experiment, whereas the positions of the E_1 and E_3 peaks are less affected. The similarity of these results to those obtained for III-V semiconductors is striking,⁸ i.e., we observe a shift of the oscillator strength toward lower energies. In particular, the E_1 intensity increases, whereas the intensities of E_2 and E_3 decrease. Accordingly, the comparison with experiment is much better when the excitonic effects are included, especially near the E_2 structure and somewhat around the E_3 structure.

It is surprising, however, that the E_1 structure is almost invisible in the Mg_2Si experimental spectrum, although it is

TABLE II. Peak positions in eV in the calculated RPA (noninteracting) and excitonic (interacting) optical spectra of Mg_2Si and Mg_2Ge compared to experiment (Ref. 16).

	Mg_2Si			Mg_2Ge		
	RPA	Interacting	Expt.	RPA	Interacting	Expt.
E_0	2.2			1.64		
E_1	2.5	2.47	2.45	2.48	2.43	2.50
E_2	3.1	2.96	2.88	3.3	3.12	3.0
E_3	3.73	3.75	3.83	3.96	4.05	4.05

already well visible at the RPA level, and much amplified in the excitonic spectrum. If we take into account the good agreement of the calculated III-V semiconductor optical spectra with experiment and the similarity of these spectra with those of Mg_2Si and Mg_2Ge , it is tempting to attribute the discrepancy between the theory and the experiment to the way the experimental spectra are extracted. Indeed, Scouler deduced the imaginary part of the dielectric function from reflectivity spectra that were measured only up to 11 eV. To perform a Kramers-Kronig transform accurately one needs to know the reflectivity spectrum up to high photon energies. To produce the high energy part of the reflectivity, Scouler used a parametrized tail to produce the continuity of the reflectivity and its correct phase factor at lower energies. Scouler recognized, however, that the positions and intensities of the peaks could be sensitive to the choice of the tail parameters. While this observation may explain the discrepancy between theory and experiment for Mg_2Ge , we do not believe that it will explain that of Mg_2Si , especially around the E_1 peak. It is thus of interest to determine the dielectric function of Mg_2Si from an ellipsometry measurement.

Conclusion. We have used our previously implemented GW approximation in conjunction with the all-electron PAW method to study the electronic structure and optical properties of Mg_2Si and Mg_2Ge . The electronic structures within

the GW approximation are in good agreement with the experimental results concerning the direct band gaps at Γ , L , and X . In addition, the GW valence bands are in excellent agreement with those obtained in the LDA, whereas the conduction bands are shifted towards higher energies by a constant energy Δ independent of the \mathbf{k} point in the Brillouin zone. We then used the shifted LDA energies to calculate the optical spectra with and without local-field and excitonic effects and found that the local-field effects drastically reduce the static dielectric function of both compounds from their LDA values in good agreement with experiment. We did not determine the effect of the excitonic effects on ϵ_∞ because our calculated real part of the dielectric function is not well converged due to the limited size of the electron-hole Hamiltonian. As for the comparison of the calculated optical spectra with experiment, as in III-V semiconductors, the excitonic effects shift the oscillator strength toward lower photon energies, and the reconstruction of the spectra is due to constructive and destructive interference phenomena caused by the mixing of electron-hole pairs in the excited wave function.

We thank P. Blöchl for providing us with his PAW code. The supercomputer time was granted by CINES on the IBM SP2 supercomputer.

-
- ¹L. Hedin, Phys. Rev. **139**, A796 (1965).
²E. Shirley, Phys. Rev. B **54**, 7758 (1996).
³R.T.M. Ummels, P.A. Bobbert, and W. van Haeringen, Phys. Rev. B **57**, 11 962 (1998).
⁴B. Farid, Philos. Mag. B **76**, 145 (1997).
⁵S. Albrecht *et al.* Phys. Rev. Lett. **80**, 4510 (1998).
⁶L.X. Benedict, E.L. Shirley, and R.B. Bohn, Phys. Rev. Lett. **80**, 4514 (1998); Phys. Rev. B **57**, R9385 (1998).
⁷M. Rohlfing and S.G. Louie, Phys. Rev. Lett. **81**, 2312 (1998).
⁸B. Arnaud and M. Alouani, Phys. Rev. B **63**, 085208 (2001).
⁹L.X. Benedict and E.L. Shirley, Phys. Rev. B **59**, 5441 (1999).
¹⁰M. Rohlfing and S.G. Louie, Phys. Rev. Lett. **82**, 1959 (1999).
¹¹J.W. van der Horst *et al.*, Phys. Rev. Lett. **83**, 4413 (1999).
¹²M. Rohlfing and S.G. Louie, Phys. Rev. Lett. **80**, 3320 (1998).
¹³E.K. Chang, M. Rohlfing, and S.G. Louie, Phys. Rev. Lett. **85**, 2613 (2000).
¹⁴M. Rohlfing *et al.*, Phys. Rev. Lett. **85**, 5440 (2000).
¹⁵J.C. Grossman *et al.*, Phys. Rev. Lett. **86**, 472 (2001).
¹⁶W.J. Scouler, Phys. Rev. **178**, 1353 (1969).
¹⁷F. Vazquez, R.A. Forman, and M. Cardona, Phys. Rev. **176**, 905 (1968).
¹⁸U. Winkler, Helv. Acta **28**, 633 (1954); P. Koenig, D.W. Lynch, and G.C. Danielson, J. Phys. Chem. Solids **20**, 122 (1961).
¹⁹G. Busch and U. Winkler, Physica (Amsterdam) **20**, 1067 (1954); L.A. Lott and D.W. Lynch, Phys. Rev. **141**, 681 (1965), and references therein.
²⁰M.Y. Au-Yang and M.L. Cohen, Phys. Rev. **178**, 1358 (1969).
²¹P.E. Blöchl, Phys. Rev. B **50**, 17 953 (1994).
²²B. Arnaud and M. Alouani, Phys. Rev. B **62**, 4464 (2000).
²³G.E. Engel and B. Farid, Phys. Rev. B **47**, 15 931 (1993).
²⁴G. Strinati, Phys. Rev. B **29**, 5718 (1984).